Analytical Methods

Accepted Manuscript

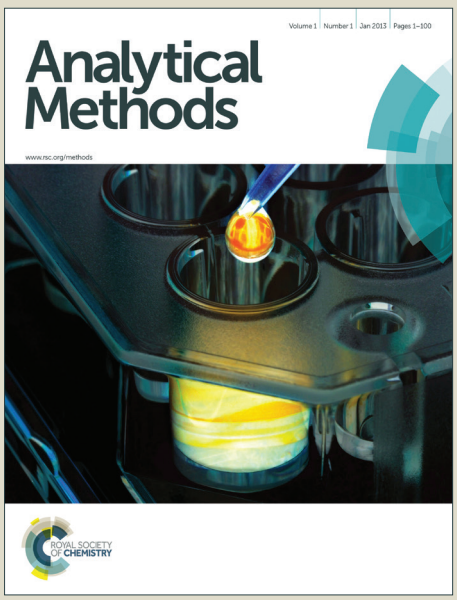

This is an *Accepted Manuscript*, which has been through the Royal Society of Chemistry peer review process and has been accepted for publication.

Accepted Manuscripts are published online shortly after acceptance, before technical editing, formatting and proof reading. Using this free service, authors can make their results available to the community, in citable form, before we publish the edited article. We will replace this *Accepted Manuscript* with the edited and formatted *Advance Article* as soon as it is available.

You can find more information about *Accepted Manuscripts* in the Information for Authors.

ROYAL SOCIETY OF CHEMISTRY

www.rsc.org/methods

An Investigation of the Conformation Changes of Myoglobin by an Electrochemical Method and a Biosensing Application Based on Controlled Protein Unfolding

Jianbo Liu[a, b], Jianbin Zheng[*a], Juncai Zhang[b], Wushuang Bai[a] and Jiangtao Liu[a]

[a] *Institute of Analytical Science/Shaanxi Provincial Key Laboratory of Electroanalytical Chemistry, Northwest University, Xi'an, Shaanxi 710069, P. R. China*

[b] *Department of Chemistry, Xianyang Normal University, Xianyang, Shaanxi 712000, P. R. China*

Abstract

The conformational changes of myoglobin (Mb) during urea-induced protein unfolding were investigated using an electrochemical method. Using several different concentrations of urea, Mb adsorbed onto a montmorillonite clay modified glassy carbon electrode (GCE) was denatured. It was determined from the relative differences in the percentage of Mb unfolding that urea-induced Mb unfolding is a one-step, two-state transition process. The results obtained using electrochemical analysis were in agreement with those obtained by UV-vis spectroscopy and fluorescence spectroscopy, confirming our observations. Thermodynamic parameters during the conformational changes were also calculated to further characterize the unfolding process of Mb. Furthermore, two typical denaturants, urea and acid, were synergistically utilized to maintain GCE incorporated Mb in its most unfolded state, while simultaneously maintaining the presence of the heme groups. Under optimal conditions, the unfolded Mb/clay/GCE exhibited accelerated direct electron transfer relative to native Mb/clay/GCE. Additionally, the sensitivity for the detection of H_2O_2

was increased nearly 10-fold, and the limit of detection (LOD) for H_2O_2 was reduced to 0.3μM for unfolded Mb/clay/GCE relative to native Mb/Clay/GCE. The present work introduces a simple and effective way to study the unfolding of metalloproteins and holds great promise for the design of novel sensitive biosensors.

Key words Electrochemistry · Conformation · Unfolding · Myoglobin · Urea

1 Introduction

During several decades, the protein folding/unfolding has been widely studied in attempts to understand the relationship between protein structure and function.[1, 2] The sequences of natural proteins have emerged through evolutionary processes so that their unique native folding states are formed very efficiently, even in the complex environment inside a living cell. However, under some conditions, proteins fail to fold correctly in living systems, and this failure can result in some amyloidoses associated diseases, including Alzheimer's disease and Parkinson's disease.[3, 4] Thus, a large number of methods have been developed to investigate protein folding/unfolding, such as UV-vis spectroscopy, fluorescence spectroscopy, circular dichroism spectroscopy, mass spectrometry, and infrared/Raman spectroscopy.[5–8]

Relative to spectral techniques, electrochemical methods play a considerable role due to their high sensitivity, rapid analysis, low instrument cost, and the capability of achieving kinetic and thermodynamic information on protein unfolding.[9–12] The electrochemical signals of proteins are closely related to the structural characteristics they possess around their redox center.[3,13–16] For instance, the relative exposure/burial

of the redox center or the disassembly/assembly of subunits within denatured protein molecules can lead to the change of peak current in voltammetry. The promotion or suppression of the electron transfer (ET) ability of the protein, which is indicative of variations in the distance between the redox center and the electrode surface, is correlated the change in peak-to-peak separation. The current-time profile provides information regarding the nature of the redox center dissociation and the dynamics of the dissociation itself.

The vast majority of proteins does not directly unfold from a natural state (N-state) to a fully unfolded state (U-state), but exist in one or more intermediate states (I-state) during the unfolding process.[17] The overall structure of these I-states are still relatively similar and contain many secondary structures, but have lost the functional activities of the original N-state. The refolding process of a protein in the U-state is roughly the reverse of the unfolding process, however, for a variety of reasons,[18] there may be different I-states that form aggregates and form precipitates. Three, four, and five states have been reported for the unfolding process of some proteins by different denaturants.[19-23] The determination of these states not only requires fluorescence spectroscopy, nuclear magnetic resonance spectroscopy, circular dichroism spectroscopy, infrared spectroscopy, size exclusion chromatography and other physical and chemical means, but also additional complex tests and complicated calculations. However, electrochemical methods also play an important role in this research. For example, our group previously reported on the stable conformational state distribution of Hemoglobin (Hb) unfolding determined by an electrochemical

method.[24]

Myoglobin (Mb) is a small heme proteins found in muscle cells whose physiological function is to store and increase the diffusion rate of dioxygen. Although Mb does not act as an electron carrier, it does participate in redox reactions in the respiratory system, thus playing an essential role in biological processes. The cofactor in native Mb is a type-b heme (iron-protoporphyrin IX ring), which directly interacts with the protein through the side chain of the proximal histidine (His93 in Mb). The second axial ligand is either exogenous water when the iron of the heme gruoups is in the ferric state, or O_2 when the iron is reduced, and both of these ligands interact with the protein through hydrogen bonding, with the distal histidine (His64 in Mb).[25] Studies on Mb folding have focused mainly on characterizing the stabilities and structures of initial, intermediate, and final apoglobin states in the absence of heme. For example, sperm whale apoMb has been shown to lose a significant amount of secondary structure after heme removal, which primarily involves unfolding of the F helix and surrounding EF and FG loops.[26–28] Further perturbation induced by the addition of heat or chemical denaturants (acid, urea, or GuHCl) leads to the complete loss of secondary and tertiary structure.

In this paper, the conformational changes occurring during the unfolding process of Mb were successfully revealed by electrochemical and optical methods. Moreover, a sensitive electrochemical approach for detecting H_2O_2 was developed based on controlled protein unfolding. This work provides a simple and effective way to study the unfolding of heme proteins, and could potentially be applied to the design of novel

and sensitive biosensors due to the greater exposure of the electrically active center relative to other methods.

2 Experimental

2.1 Chemicals and reagents

Bovine Mb (M_w = 17 700) was purchased from Sigma and used without further purification. Urea was obtained from Fluka. Other reagents were analytical reagent grade.

Phosphate buffer saline (PBS, 0.1 M, pH 7.0, containing 0.1 M KCl) was prepared from the stock solutions of Na_2HPO_4 and NaH_2PO_4, and adjusted to the pH value. Urea solutions with different concentrations (1.0-8.0 M) were prepared by dissolving desirable amount of urea in PBS. Montmorillonite clay suspension (1.0 mg mL^{-1}) was prepared by dispersing clay (1.0 mg) in doubly distilled water (1.0 mL) with ultrasonication before use.

2.2 Electrochemical measurements

A glassy carbon electrode (GCE) of 3 mm diameter was polished to a mirror-like state with 1.0, 0.3 and 0.05 mm Al_2O_3 powder. The well polished GCE was cleaned in absolute ethanol and doubly distilled water by sonication for 5 min, respectively. Montmorillonite clay suspension (5 μL) was then carefully dropped onto the surface of GCE and dried at room temperature (clay/GCE). Mb was dissolved in PBS solution,

and the Mb concentration was 5 mg mL^{-1}; 5 μL of the resulting solution was cast onto the clay/GCE surface using a syringe. The modified electrode was moved into a refrigerator and kept at 4 °C to dry overnight. The fabricated modified electrode was stored at 4 °C in a refrigerator when not in use and noted as Mb/clay/GCE. Mb/clay/GCE was dipped in different concentration of urea (1.0-8.0 M) at 4 °C for 8 h to make Mb unfold in different levels.

Cyclic voltammetry (CV) was performed with CHI 660D electrochemical workstation (Shanghai CH Instrument Co. Ltd., China) in three-electrode cell. Modified GCE was used as working electrode, and a platinum spiral wire was used as the counter electrode. All potentials were biased versus saturated calomel electrode (SCE). For the electrochemical experiments conducted under anaerobic conditions, the solutions were bubbled with pure N_2 gas for more than 30 min, and N_2 gas was kept flowing over the solution during the electrochemical measurements.

2.3 Spectral measurements

UV-vis absorption spectra were recorded on a Specord 50 spectrometer (Jena, Germany). Fluorescence measurements were conducted on an F-2500 fluorescence spectrometer with xenon lamps (Hitachi Ltd., Japan). Unless stated otherwise, all measurements were performed at ambient temperature (25 ± 2 °C).

For all spectral measurements, Mb was incubated in urea (1.0-8.0 M) for 8 h at 4 °C to reach equilibrium, and the unfolded Mb was noted as uMb. In order to obtain better spectra, all the Mb solutions were diluted before measurements, and the time

between the measurements and dilution was controlled within seconds. The concentrations of Mb for UV-vis and fluorescence measurements were 80 and 300 mg L^{-1}, respectively. Some parameters fluorescence measurements are listed below. The slits of excitation and emission were both 5 nm; the excitation wavelength was 295 nm; the scanning range of wavelength was 300-450 nm; the scanning speed was 1000 nm / min. All spectral measurements were carried out at ambient temperature (25 ± 2 °C).

3 Results and Discussion

3.1 Effect of unfolding time

The effect of unfolding time on Mb induced by urea was investigated firstly. Fig. 1 showed the variation of absorbance and fluorescence intensity during Mb unfolding induced by 8.0 M urea from 1 h to 12 h. The absorbance decreased gradually while fluorescence intensity increased from 1 h to 8 h, which revealed the change of Mb conformation. The absorbance and fluorescence intensity kept almost the same beyond 8 h, which showed that the conformation of Mb was stable. Therefore, the time of unfolding for Mb induced by urea was determined for 8 h.

Fig. 1

3.2 Urea-induced unfolding of Mb on clay-modified electrode

In the native state of Mb, the iron atom in the center of heme porphyrin has six coordinate bonds, four of which participate in the coordination with the nitrogen atoms in porphyrin ring and form a plane. The heme groups are deeply buried in the hydrophobic pockets of Mb with a six-coordinate high-spin complex and thus show a poor electrochemical property at modified electrode. Mb and Hb are both belong to hemeproteins, our previous research[24] showed that the electrochemical response increased upon the unfolding of Hb induced by urea because of the exposure of electrical active center.

Fig. 2A showed typical cyclic voltammograms (CVs) of different chemically modified electrode in the absence or presence of 8.0 M urea as the denaturant. Clay had no electrochemical response on GCE (Fig. 2A, curve a), after Mb adsorbed onto the clay/GCE (Mb/clay/GCE), a pair of weak redox peaks were observed with the formal potential ($E^{o'}$) of −0.208 V and the peak-to-peak separation (ΔE_p) of 112 mV (Fig. 2A, curve b). The redox couple at −0.208 V was attributed to the redox reaction of heme Fe^{III}/Fe^{II} in Mb.[29] The $E^{o'}$ of Mb was smaller than previous reports that Mb was immobilized in Cys/Au,[30] and Chit-MWCNT/AgNPs/GCE.[31] This indicates that the different film components, which might interact with protein or affect electric double layer of the electrode, may have an obvious effect on the kinetics of the electrode reaction for hemeproteins.[32, 33] Mb is one of the most well-studied proteins and has long been serving as a model for the folding and unfolding of heme proteins. The long distance between the heme groups and electrode and the large steric hindrance of native Mb[34] essentially result in the poor electrochemical response of Mb

at the clay modified GCE. The incubation of Mb in 8.0 M urea (uMb/clay/GCE) caused changes of the native secondary and tertiary structure surrounding the heme group, thus resulted an enhancement of the water solubility of hydrophobic side chains. Therefore, the peak current (I_p) increased greatly with a positive shift of $E^{o'}$ to -0.182 V and an enlarged ΔE_p to 183 mV (Fig. 2A, curve c). The change of the coordinating environment of heme irons resulted in the change of $E^{o'}$.[35] Although the direct electron transfer between the heme groups of Mb and clay-related film can be facilitated, the ΔE_p was larger than that of Mb/clay/GCE, moreover, the I_p of uMb/clay/GCE was larger than that of Mb/clay/GCE, suggesting that the greater exposure of the electroactive center and the change of Mb conformation.

Fig. 2

The hydrogen bonds formed by urea and amino acid residues in the protein have an important role for the protein unfolding, and different concentration of urea can cause different exposure extent of electrical active center in Mb. Fig. 2B showed the CVs of Mb which was unfolded by urea with different concentrations. The current response increased at different extent as urea concentration increased because of the greater exposure of the electroactive center. Fig. 2C showed the relationship between I_{pc} and urea concentration during the step-wise denaturation of Mb. The change for I_{pc} was great as urea concentration between 0-3.0 M, which indicated that the conformation of Mb changed greatly. I_{pc} changed slightly as urea concentration from

3.0 to 8.0 M.

The Söret absorption band (350-450 nm) of hemeprotein is sensitive to conformation change nearby heme.[36, 37] Therefore, UV-vis absorption spectrum is widely used for the research of Mb conformation change.

Without the presence of urea, a tight Söret band at 410 nm was obtained (Fig. 3, curve a), which was assigned to the heme monomer coordinated to His93 in the native state of Mb.[36] The intensity of the absorption spectra decreased as the urea concentration from 1.0 M to 8.0 M (curves b-i). Moreover, the maximum absorption wavelength kept almost the same under various urea concentrations, indicating the heme remained attached to Mb at the native site when Mb was unfolded by urea.[38] The Söret absorption band of hemeprotein is caused by the interaction between heme and globin. In urea-water mixture, the hydrogen bond between urea and globin can effect the interaction and result in the decrease of absorption intensity.[34]

Fig. 3

The intrinsic fluorescence property of proteins has proved to be a useful probe of protein structure, function, and dynamic. Tryptophan (Trp), tyrosine and phenylanine amino acid residues in protein molecules emit fluorescence. As shown in Fig. 4, the Mb molecule produced a maximum emission peak at 346 nm (curve a). When the urea concentration increased from 1.0 to 8.0 M, the fluorescence intensity of Trp increased gradually, and the maximum emission wavelength shifted slightly to 357

nm (curves b-i), indicating that the presence of urea caused changes of hydrophobicity in the vicinity of Trp residues. In native Mb, the Trp residues are located in the vicinity of heme, and their fluorescence is strongly quenched by Förster resonance energy transfer.[39, 40] With the increase of urea concentration, the conformational change of Mb led to the increase of the distance between Trp and heme. Accordingly, the energy transfer efficiency was reduced, and the fluorescence intensity increased gradually.[7, 41]

Fig. 4

In order to further evaluate the results from different techniques, a linear free energy model (LEM) was used.[42, 43]

$$f_U\,(\%) = \frac{y - y_N}{y_U - y_N} \times 100\% \quad \text{(for CV and Fluorescence spectroscopy)} \qquad (1)$$

$$f_U\,(\%) = \frac{y_N - y}{y_N - y_U} \times 100\% \quad \text{(for UV-vis spectroscopy)} \qquad (2)$$

Where y represents the electrochemical or spectral intensity value in a particular unfolding condition, y_N and y_U are the electrochemical or spectral intensity value in the native and fully unfolded state of Mb. The unfolded percentage of the native Mb (f_N) is 0 % while that of the fully unfolded Mb (f_U) is 100 %.

Fig. 5 summarized the results obtained by electrochemistry, UV-vis spectroscopy, and fluorescence spectroscopy for Mb unfolding as a function of the urea denaturant. The unfolding percentage of Mb obtained by the three methods was calculated by

using the value obtained in the absence or presence of urea. The small discrepancies of f_U from electrochemistry and spectroscopy methods was because electrochemical measurements were performed on the electrode interface, while spectral measurements in solution system. There was no platform in f_U during the Mb unfolding induced by urea, consequently, a one-step, two-state transition process was monitored by electrochemical and spectral methods. This showed that there were only two stable conformations, including natural state and completely unfolded state. The denatu- ration process of Mb conformed to a typical two-state model. In our previous research, there existed an intermediate state in Hb step-wise unfolding induced by urea, however, no intermediate state was found in Mb unfolding induced by urea. The possible reason is that the molecular structure of Mb is different from Hb. Hb in its native state is approximately spherical in shape with dimensions of 65 × 55 × 50 Å and has a heterotetrameric structure composed of four subunits that are referred to as α1 and α2 subunits with eight helices and β1 and β2 subunits with seven helices. However, the molecule structure of Mb is relatively simple than that of Hb. Mb is a small, compact globular protein having eight α helices (A-H) and is composed of 153 amino acids cradling a heme prosthetic group with iron in center surrounded by a hydrophobic core. The good consistency in the unfolding curves obtained with CV, UV-vis spectroscopy and fluorescence spectroscopy further substantially validated the electrochemical method based on the redox process of the heme groups at chemical modified electrodes as a new tool for the study of the unfolding processes of Mb induced by urea.

Fig. 5

3.3 The calculation of the thermodynamic parameters during Mb conformational change

According to the LEM,[42, 43] the relationship between the free energy and equilibrium constant is shown as following:

$$K_{eq} = \frac{f_U}{f_N} = \frac{f_U}{1 - f_U} \qquad (3)$$

$$\Delta G_U = -RT \ln K_{eq} \qquad (4)$$

$$\Delta G_U = \Delta G_{U,\,water} - m[D] \qquad (5)$$

K_{eq} is the equilibrium constant between the folded and unfolded state of Mb. ΔG_U is the change in the free energy of Mb in a certain unfolding condition. $\Delta G_{U,\,water}$ is the change in the free energy of the folding Mb in water. m, which can index the change in solvent exposure during the transition and the compactness of Mb, is obtained from the slope of the Santoro-Bolen equation.[44–46] [D] is the concentration of urea. Accordingly, similar thermodynamic parameters of m and $\Delta G_{U,\,water}$ of Mb were obtained from electrochemistry, fluorescence spectroscopy and UV-vis spectroscopy (Table 1).

Table 1

The small discrepancies of m and $\Delta G_{U,water}$ from electrochemistry and

spectroscopy methods was also due to that electrochemical measurements were performed on the electrode interface, while spectral measurement in solution system.

A thermodynamic cycle of Mb induced by urea was established as following:[47, 48]

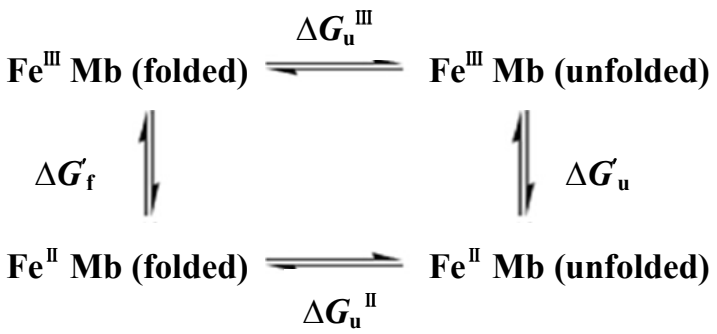

By combining the electrochemical data with the free energy changes in Mb unfolding process, the different stability of reduced and oxidized Mb induced by urea can be assessed from the cycle. According to $\Delta G_f' - \Delta G_u' = -nF\,(\Delta E^{o'}) = -nF\,(E_f^{o'} - E_u^{o'})$, the difference of the free energies between unfolding the oxidized and the reduced Mb ($\Delta\Delta G_u = \Delta G_u^{III} - \Delta G_u^{II}$) was estimated to be −3.5 kJ mol^{-1}. Consequently, when treated with urea at pH 7.0, the reduced Fe^{II} Mb was more stable than the oxidized Fe^{III} Mb, which may be caused by the different coordination environments of Fe^{II} and Fe^{III} in the native Mb.

3.4 Optimization of Mb unfolding conditions

Protein controllable unfolding can be used for biosensor establishment with high sensitivity because of the greater exposure of the electroactive center.[49] As typical denaturants, acid and urea have different unfolding ability. Acid has strong subunit and heme-dissociating ability, while urea has chaotropic effects.[28] By synchronous

optimization of acid and urea conditions, the unfolding state of Mb can be precisely regulated to a most unfolded state without losing the heme groups in 5.0 M urea at pH 4.0. Fig. 3 showed the UV-vis spectra of 80 mg L^{-1} Mb in 0.1 M pH 7.0 PBS containing different concentrations of urea from 0 to 8.0 M. Mb in neutral PBS exhibited a sharp Söret absorption at 410 nm, which is attributed to he heme monomer coordinated to His93. As urea increased from 1.0 to 8.0 M, the intensity of the Söret absorption decreased markedly at nearly a constant maximal absorption wavelength. The results suggested that urea is a mild denaturant and Mb only undergoes conformational changes while does not lose its heme groups even at high concentration of urea.[50]

In comparison with the unfolding of Mb by urea, Mb in 0.1 M PBS with different pH from 7.0 to 1.0 showed different unfolding behaviors (Fig. 6A). The Söret absorption at 410 nm showed no obvious change at pH from 7.0 to 5.0, and a dramatic decrease at pH 4.0. When pH lower than 4.0, the Söret absorption at 410 nm totally disappeared and a new broad Söret band near 392 nm emerged, indicating the rupture of the coordination bond between heme groups and the His93 of Mb.

In order to mostly expose Mb without losing its heme groups, acid and urea were performed synchronously. Fig. 6B showed the UV-vis spectra of 80 mg L^{-1} Mb in 5.0 M urea solution with various pH values. With decrease in pH from 6.0 to 4.0, the Söret absorbance of Mb at 410 nm dramatically decreased with no shift in the maximal absorption wavelength. When pH was lower than 4.0, the absorption peak at

390 nm appeared and increased with the decrease in pH, suggesting the start of breaking the heme groups in Mb. These results indicate that Mb in pH 4.0 PBS containing 5.0 M urea can be exposed mostly without losing heme groups.

The unfolding state of Mb in 5.0 M urea with different pH values was also investigated by fluorescence spectroscopy, as shown in Fig. 6C. When pH gradually decreased from 6.0 to 4.0, the fluorescence enhanced dramatically with red shift. Mb molecule contains a number of Trp residues, which locate closely to heme groups. The fluorescence emission spectrum of Trp residues, which is quenched by heme and other surrounding groups in native Mb, reflects the conformational information of Mb. The unfolding of Mb increases the distance between Trp residues and heme groups. Therefore, the energy transfer between Trp residues and heme groups decreases accordingly,[13] causing the enhancement of the fluorescence intensity. Besides, the exposure of Trp residues to polar environment with the unfolding of Mb results in the red shift of Trp fluorescence.[3] When pH decreased to 4.0, the fluorescence intensity reached the maximum and leveled off, indicating the completely exposed state of Mb. Further reduce of pH led to a dramatic decrease in fluorescence intensity, suggesting the start losing of heme groups. Consequently, in order to obtain the best electrocatalytic activity, an unfolding condition of pH 4.0 PBS containing 5.0 M urea was selected.

Fig. 6

3.5 Electrocatalytic ability of unfolded Mb/clay/GCE based on controlled protein unfolding

Amperometric detection is an important detection method in electrochemical analysis. The resulting current is proportional to the concentration of the species generating the current, and the quantification of H_2O_2 can be achieved via the electrochemical detection of the proposed Mb modified electrode.

The response of the modified electrode for determination of H_2O_2 based on uMb/clay/GCE was tested by the amperometric current-time curves. Fig. 7 demonstrated the typical current-time curves of this modified electrode through successive addition H_2O_2 of different concentration into a 20 mL continuous stirring N_2-saturated PBS. When H_2O_2 was added into 0.1 M blank PBS, the reduction current rose steeply to reach a stable value. The 95% of the steady-state current could be obtained at about 3 s by using the proposed modified electrode, which indicated a fast response process. In addition, the current responses of the proposed modified electrode were linearly related to H_2O_2 concentration in a wider linearity range from 8.0×10^{-7} to 1.8×10^{-4} M (inset in Fig.7). The linear regression equation is I (μA) = 4.73×10^{-2} C (μM) + 8.42×10^{-3} (r = 0.9983) with a limit of detection (LOD) 3.0×10^{-7} M (S/N = 3). A sensitivity of 151.5 μA mM^{-1} was obtained, which was nearly 10-fold larger than that of neutral Mb/clay/GCE (15.5 μA mM^{-1}, inset in Fig.7). The great improvements in sensitivity and LOD hold great promise for the design of novel sensitive biosensors. Moreover, the performance comparisons of the present sensor with others were presented in Table 2. Through these comparisons, obviously,

performance of the uMb/clay/GCE was better than that of other electrodes, especially the extremely high sensitivity and low LOD. The high sensitivity and low LOD were due to the greater exposure of the electrical active center of hemeprotein with the denaturant and the acceleration of electron transfer.

The cyclic voltammetric responses of the uMb/clay/GCE in PBS retained above 98% of its initial response after 30 cycles, and then it decreased slowly with the increase of the cycle, indicating that the modfied electrode was stable. The storage stability of the uMb/clay/GCE was further investigated. The amperometric measurements were measured using the same electrode and it retained above 96% of its initial response after being stored at 4 °C for one months. These results displayed that the sensor had a good stability.

Fig. 7

Table 2

Conclusions

An effective electrochemical method was successfully demonstrated here for investigation of conformation change of Mb during its unfolding induced by urea. The results showed that there were only two stable conformations, including natural state and completely folded state during Mb unfolding process induced by urea. In order to overcome the obstacles of low sensitivity and long response time of routine methods,

the entrapped Mb in Mb/clay/GCE was controlled to the most unfolding state, and the electrocatalytic ability of Mb/clay/GCE was extremely improved. The method demonstrated here could provide a simple and effective way to research hemeprotein unfolding and present new idea for the novel sensitive biosensors design based on the greater exposure of the electrical active center of hemeprotein with the denaturant.

Acknowledgements

The authors gratefully acknowledge the financial support of this project by the National Natural Science Foundation of China (NO. 21275116, 21305117), the Specialized Research Fund for the Doctoral Program of Higher Education of China (NO. 20126101120023), the Natural Science Foundation of Shaanxi Province of China (NO. 2012JM2013, 2012JQ2014) and the Scientific Research Foundation of Shaanxi Provincial Key Laboratory (2010JS088, 11JS080, 12JS087, 13JS097).

References

1. C. M. Dobson, Protein folding and misfolding, *Nature*, 2003, **426**, 884–890.
2. N. Go, Theoretical studies of protein folding, *Annu. Rev. Biophys. Bioeng.*, 1983, **12**, 183–210.
3. X. C. Li, W. Zheng, L. M. Zhang, P. Yu, Y. Q. Lin, L. Su and L. Q. Mao, Effective electrochemical method for investigation of hemoglobin unfolding based on the redox property of heme groups at glassy carbon electrodes, *Anal. Chem.*, 2009, **81**, 8557–8563.

4. A. L. Fink, Protein aggregation: folding aggregates, inclusion bodies and amyloid, *Folding Des*., 1998, **3**, R9–R23.

5. M. Fedurco, J. Augustynski, C. Indiani, G. Smulevich, M. Antalik, M. Bano, E. Sedlak, M. C. Glascock and J. H. Dawson, The heme iron coordination of unfolded ferric and ferrous cytochrome c in neutral and acidic urea solutions. Spectroscopic and electrochemical studies, *Biochim. Biophys. Acta*, 2004, **1703**, 31–41.

6. W. P. Griffith and I. A. Kaltashov, Highly asymmetric interactions between globin chains during hemoglobin assembly revealed by electrospray ionization mass spectrometry, *Biochemistry*, 2003, **42**, 10024–10033.

7. M. C. Kuprowski, B. L. Boys and L. Konermann, Analysis of protein mixtures by electrospray mass spectrometry: effects of conformation and desolvation behavior on the signal intensities of hemoglobin subunits, *J. Am. Soc. Mass Spectrom*., 2007, **18**, 1279–1285.

8. C. W. Liu, A. L. Bo, G. J. Cheng, X. Q. Lin and S. J. Dong, Characterization of the structural and functional changes of hemoglobin in dimethyl sulfoxide by spectroscopic techniques, *Biochim. Biophys. Acta*, 1998, **1385**, 53–60.

9. L. H. Guo and N. Qu, Chemical-induced unfolding of cofactor-free protein monitored by electrochemistry, *Anal. Chem*., 2006, **78**, 6275–6278.

10. M. Fedurco, J. Augustynski, C. Indiani, G. Smulevich, M. Antalik, M. Bano, E. Sedlak, M. C. Glascock and J. H. Dawson, Electrochemistry of unfolded cytochrome c in neutral and acidic urea solutions, *J. Am. Chem. Soc*., 2005, **127**,

7638–7646.

11. J. Bixler, G. Bakker and G. McLendon, Electrochemical probes of protein folding, *J. Am. Chem. Soc*., 1992, **114**, 6938–6939.

12. P. Wittung-Stafshede, M. G. Hill, E. Gomez, A. J. Di Bilio, B. G. Karlsson, J. Leckner, J. R. Winkler, H. B. Gray and B. G. Malmstrçm, Reduction potentials of blue and purple copper proteins in their unfolded states: a closer look at rack induced coordination, *J. Biol. Inorg. Chem*., 1998, **3**, 367–370.

13. Z. B. Mai, X. J. Zhao, Z. Dai and X. Y. Zou, Contributions of components in guanidine hydrochloride to hemoglobin unfolding investigated by protein film electrochemistry, *J. Phys. Chem. B*, 2010, **114**, 7090–7097.

14. C. X. Cai and J. Chen, Direct electron transfer of glucose oxidase promoted by carbon nanotubes, *Anal. Biochem*., 2004, **332**, 75–83.

15. C. X. Cai and J. Chen, Direct electron transfer and bioelectrocatalysis of hemoglobin at a carbon nanotube electrode, *Anal. Biochem*., 2004, **325**, 285–292.

16. C. Y. Lee and A. M. Bond, A comparison of the higher order harmonic components derived from large-amplitude Fourier transformed ac voltammetry of myoglobin and heme in DDAB Films at a pyrolytic graphite electrode, *Langmuir*, 2010, **26**, 5243–5253.

17. B. M. Gorovits, W. A. McGee and P. M. Horowitz, Rhodanese folding is controlled by the partitioning of its folding intermediates, *Biochim. Biophys. Acta*, 1998, **1382**, 120–128.

18. I. M. Kuznetsova, K. K. Turoverov and V. N. Uversky, Use of the phase diagram method to analyze the protein unfolding-refolding reactions: fishing out the "Invisible" intermediates, *J. Proteome. Res*., 2004, **3**, 485–494.

19. R. F. Latypov, H. Cheng, N. A. Roder, J. R. Zhang and H. Roder, Structural characterization of an equilibrium unfolding intermediate in cytochrome c, *J. Mol. Biol.*, 2006, **357**, 1009–1025.

20. V. N. Uversky, N. V. Narizhneva, S. O. Kirschstein, S. Winter and G. Lober, Conformational transitions provoked by organic solvents in β-lactoglobulin: can a molten globule like intermediate be induced by the decrease in dielectric constant? *Folding Des.*, 1997, **2**, 163–172.

21. V. N. Uversky and O. B. Ptitsyn, Further evidence on the equilibrium "Pre-molten globule state": four-state guanidinium chloride-induced unfolding of carbonic anhydrase B at low temperature, *J. Mol. Biol.*, 1996, **255**, 215 –228.

22. V. N. Uversky and O. B. Ptitsyn, "Partly folded" state, a new equilibrium state of protein molecules: Four-state guanidinium chloride-induced unfolding of beta-lactamase at low temperature, *Biochemistry*, 1994, **33**, 2782–2791.

23. I. M. Kuznetsova, O.V. Stepanenko and K. K. Turoverov, Unraveling multistate unfolding of rabbit muscle creatine kinase, *Biochim. Biophys. Acta*, 2002, **1596**, 138–155.

24. J. B. Liu, Y. Dong, J. B. Zheng, Y. P. He and Q. L. Sheng, Investigation on the conformation change of hemoglobin immobilized on MPA-modified electrode by electrochemical method, *Anal. Sci.*, 2013, **29**, 1075–1081.

25. M. L. Quillin, R. M. Arduini, J. S. Olson, and G. N. Jr, High-resolution crystal structures of distal histidine mutants of sperm whale myoglobin, *J. Mol. Biol.*, 1993, **234**, 140–155.

26. D. Eliezer and P. E. Wright, Is apomyoglobin a molten globule? Structural characterization by NMR, *J. Mol. Biol*., 1996, **263**, 531–538.

27. M. J. Cocco and J. T. Lecomte, Characterization of hydrophobic cores in apo-myoglobin: A proton NMR spectroscopy study, *Biochemistry*, 1990, **29**, 11067–11072.

28. F. M. Hughson, P. E. Wright and R. L. Baldwin, Structural characterization of a partly folded apomyoglobin intermediate, *Science*, 1990, **249**, 1544–1548.

29. Y. P. He, D. W. Zhang, S. Y. Dong and J. B. Zheng, A novel nitrite biosensor based on gold dendrites with egg white as template, *Anal. Sci*., 2012, **28**, 403–409.

30. T. Paulo, I. C. N. Diógenes and H. D. Abruña, Direct electrochemistry and electrocatalysis of myoglobin immobilized on l-cysteine self-assembled gold electrode, *Langmuir*, 2011, **27**, 2052–2057.

31. Y. C. Li, Y. J. Li and Y. Y. Yang, Direct electrochemistry and electrocatalysis of myoglobin-based nanocomposite membrane electrode, *Bioelectrochem*., 2011, **82**, 112–116.

32. J. F. Rusling, Enzyme bioelectrochemistry in cast biomembrane-like films, *Acc Chem. Res*., 1998, **31**, 363–369.

33. G. Zhao, J. J. Feng, J. J. Xu and H. Y. Chen, Direct electrochemistry and electrocatalysis of heme proteins immobilized on self-assembled ZrO_2 film, *Electrochem. Commun*., 2005, **7**, 724–729.

34. D. S. Culbertson and J. S. Olson, Role of heme in the unfolding and assembly of

myoglobin, *Biochemistry*, 2010, **49**, 6052–6063.

35. C. J. Reedy, M. M. Elvekrog and B. R. Gibney, Development of a heme protein structure-electrochemical function database, *Nucleic. Acids. Res*., 2008, **36**, D307 –D313.

36. B. L. Boys, M. C. Kuprowski and L. Konermann, Symmetric behavior of hemoglobin α- and β-subunits during acid-induced denaturation observed by electrospray mass spectrometry, *Biochemistry*, 2007, **46**, 10675–10684.

37. S. Devineau, J. M. Zanotti, C. Loupiac, L. Zargarian, F. Neiers, S. Pin and J. P. Renault, Myoglobin on Silica: A case study of the impact of adsorption on protein structure and dynamics, *Langmuir*, 2013, **29**, 13465–13472.

38. X. J. Zhao, Z. B. Mai, Z. Dai and X. Y. Zou, Direct probing of the folding/unfolding event of bovine hemoglobin at montmorillonite clay modified electrode by adsorptive transfer voltammetry, *Talanta*, 2011, **84**, 148–154.

39. D. Patra and C. Barakat, Time-resolved fluorescence study during denaturation and renaturation of curcumin-myoglobin complex, *Int. J. Biol. Macromol*., 2012, **50**, 885–890.

40. A. Malik, J. Kundu, S. Mukherjee and P. Chowdhury, Myoglobin unfolding in crowding and confinement, *J. Phys. Chem. B*, 2012, **116**, 12895–12904.

41. M. O. Crespin, B. L. Boys and L. Konermann, The reconstitution of unfolded myoglobin with hemin dicyanide is not accelerated by fly-casting, *FEBS Lett*., 2005, **579**, 271–274.

42. C. N. Pace, The stability of globular protein, *Crit Rev. Biochem. Mol. Biol*., 1975,

3, 1–43.

43. J. A. Schellman, Solvent denaturation, *Biopolymers*, 1978, **17**, 1305–1322.

44. R. A. Staniforth, M. G. Bigotti, F. Cutruzzol, C. T. Allocatelli and M. Brunori, Unfolding of apomyoglobin from Aplysia limacina: the effect of salt and ph on the cooperativity of folding, *J. Mol. Biol*., 1998, **275**, 133–148.

45. D. O. V. Alonso and K. A. Dill, Solvent denaturation and stabilization of globular proteins, *Biochemistry*, 1991, **30**, 5974–5985.

46. M. J. Parker, J. Spencer and A. R. Clarke, An integrated kinetic analysis of intermediates and transition states in protein folding reactions, *J. Mol. Biol*., 1995, **253**, 771–786.

47. D. Elbaum, E. R. Pandolfelli and T. T. Herskovits, Denaturation of human and Glycera dibranchiata hemoglobins by the urea and amide classes of denaturants, *Biochemistry*, 1974, **13**, 1278–1284.

48. K. Kawahara, A. G. Kirshner and C. Tanford, Dissociation of human Co-hemoglobin by urea, guanidine hydrochloride, and other reagents, *Biochemistry*, 1965, **4**, 1203–1213.

49. H. Wu, S. H. Fan, W. Y. Zhu, Z. Dai and X. Y. Zou, Investigation of electrocata-lytic pathway for hemoglobin toward nitric oxide by electrochemical approach based on protein controllable unfolding and in-situ reaction, *Biosens. and Bioelectron*., 2013, **41**, 589-594.

50. Q. Shao, P. Wu, P. Gu, X. Q. Xu, H. Zhang and C. X. Cai, Electrochemical and spectroscopic studies on the conformational structure of hemoglobin assembled

on gold nanoparticles, *J. Phys. Chem. B*, 2011, **115**, 8627– 8637.

51. S. Komathi, A. L. Gopalan, S. K. Kim, G. S. Anand and K. P. Lee, Fabrication of horseradish peroxidase immobilized poly (N-[3-(trimethoxy silyl)propyl]aniline) gold nanorods film modified electrode and electrochemical hydrogen peroxide sensing, *Electrochim. Acta*, 2013, **92**, 71–78.
52. P. R. Solanki, A. Kaushik, A. A. Ansari, G. Sumana and B. D. Malhotra, Horse radish peroxidase immobilized polyaniline for hydrogen peroxide sensor, *Polym. Adv. Technol*., 2011, **22**, 903–908.
53. G. Zhao, J. J. Xu and H.Y. Chen, Interfacing myoglobin to graphite electrode with an electrodeposited nanoporous ZnO film, *Anal. Biochem*., 2006, **350**, 145–150.
54. Y. P. He, Q. L. Sheng, J. B. Zheng, M. Z. Wang and B. Liu, Magnetite-graphene for the direct electrochemistry of hemoglobin and its biosensing application, *Electrochim. Acta*, 2011, **56**, 2471–2476.
55. W. Sun, X. Q. Li, P. Qin and K. Jiao, Electrodeposition of Co nanoparticles on the carbon ionic liquid electrode as a platform for myoglobin electrochemical biosensor, *J. Phys. Chem. C*, 2009, **113**, 11294–11300.
56. W. Sun, D. D. Wang, R. F. Gao and K. Jiao, Direct electrochemistry and electrocatalysis of hemoglobin in sodium alginate film on a BMIMPF6 modified carbon paste electrode, *Electrochem. Commun*., 2007, **9**, 1159–1164.
57. Y. Zhang and J. B. Zheng, Direct electrochemistry and electrocatalysis of myoglobin immobilized in hyaluronic acid and room temperature ionic liquids composite film, *Electrochem. Commun*., 2008, **10**, 1400–1403.

58. C. F. Ding, M. L. Zhang, F. Zhao and S. S. Zhang, Disposable biosensor and biocatalysis of horseradish peroxidase based on sodium alginate film and room temperature ionic liquid, *Anal. Biochem*., 2008, **378**, 32–37.

Captions

Fig. 1 Effect of spectral intensity toward unfolding time. (A) The relation curve between the max absorbance in UV-vis spectra and unfolding time. (B) The relation curve between the max fluorescence intensity and unfolding time. The Mb was unfolded in 8.0 M urea solution.

Fig. 2 （A）CVs of clay/GCE (a), Mb/clay/GCE (b), and uMb/clay/GCE (c) in pH 7.0 PBS at scan rate of 0.3 V s^{-1}. （B）The CVs of uMb/clay/GCE, in which Mb was unfolded by 1.0, 2.0, 3.0, 4.0, 5.0, 6.0, 7.0 and 8.0 M urea, respectively (from a to h). The scan rate was 0.3 V s^{-1}. （C）The relationship between I_{pc} on clay-modified electrode and the concentration of urea.

Fig. 3 UV-vis spectra of Mb incubated in the presence of 0, 1.0, 2.0, 3.0, 4.0, 5.0, 6.0, 7.0 and 8.0 M urea (a to i). The concentration of Mb was 80 mg L^{-1}.

Fig. 4 The intrinsic fluorescence emission spectra of Trp within Mb unfolded by 0, 1.0, 2.0, 3.0, 4.0, 5.0, 6.0, 7.0 and 8.0 M urea, respectively (a to i). The concentration of Mb was 300 mg L^{-1}. The excitation wavelength was 295 nm.

Fig. 5 The unfolding curves of Mb obtained from CV (■), molecule fluorescence spectroscopy (MFS) (▲) and UV-vis absorbance (▼) changes resulting from the unfolding of Mb induced by different concentrations of urea.

Fig. 6 (A) UV-vis spectra of 80 mg L^{-1} Mb in 0.1 M PBS with different pH values of 7.0, 6.0, 5.0, 4.0, 3.0, 2.0, and 1.0 (a to g). (B) UV-vis spectra of 80 mg L^{-1} Mb in 5.0 M acidic urea with various pH values of 6.0, 5.0, 4.0, 3.0, 2.0, and 1.0. (C) fluorescence spectra of 300 mg L^{-1} Mb in 5.0 M acidic urea with various pH values of 6.0, 5.0, 4.0, 3.0, 2.0, and 1.0.

Fig. 7 Amperometric responses of the uMb/clay/GCE at −100 mV (vs. SCE) upon successive addition of H_2O_2 into a deoxygenated 0.1 M PBS (pH 7.0); inset: plot of catalytic current vs. H_2O_2 concentration. The black bars represent the unfolded Mb/clay/GCE, while red bars represent the natural Mb/clay/GCE.

Table 1 The comparisons of m, and $\Delta G_{U,\ water}$ obtained from electrochemical, fluorescence and UV-vis.

Table 2 Comparison of the developed H_2O_2 biosensor with other enzymatic H_2O_2 biosensors.

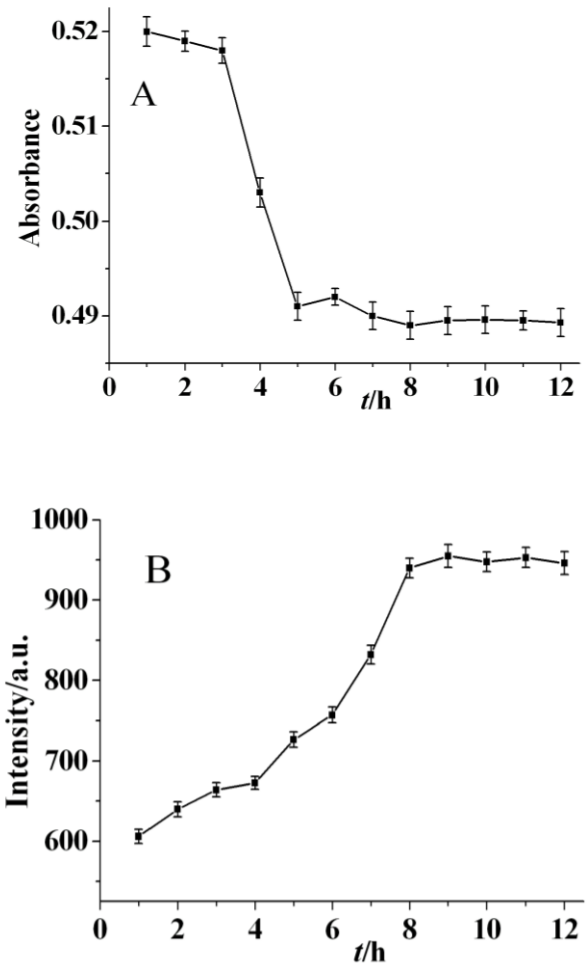

Fig. 1

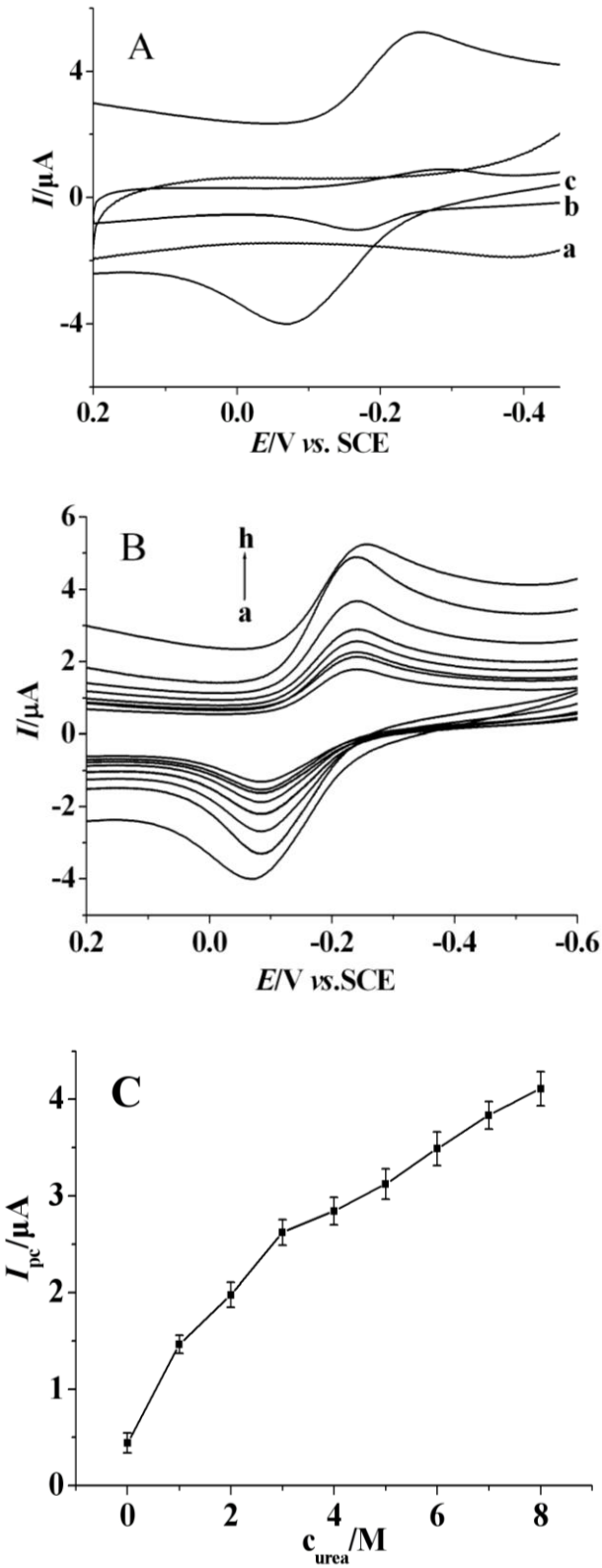

Fig. 2

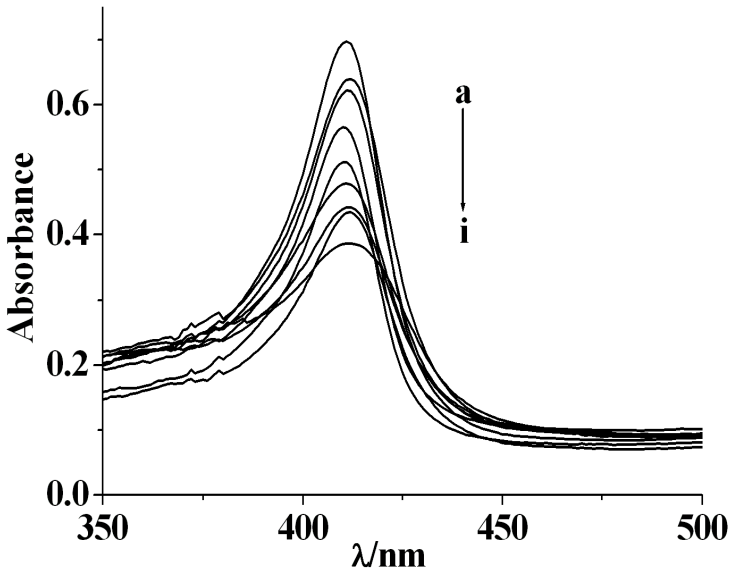

Fig. 3

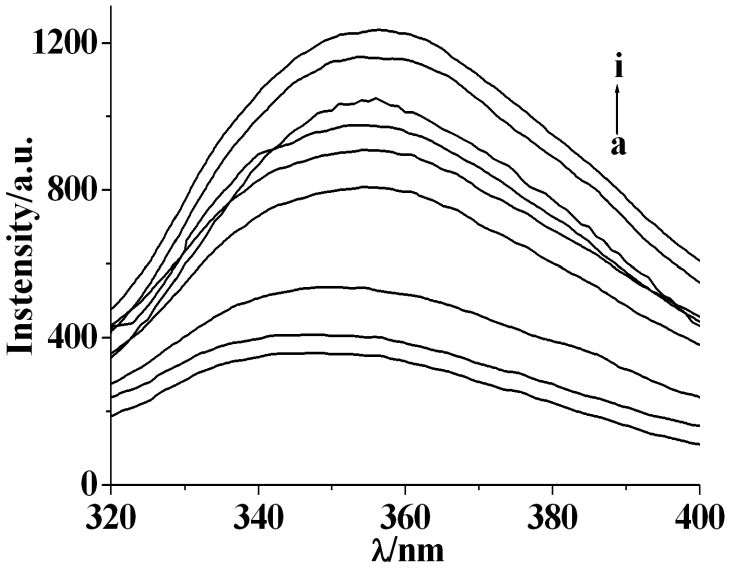

Fig. 4

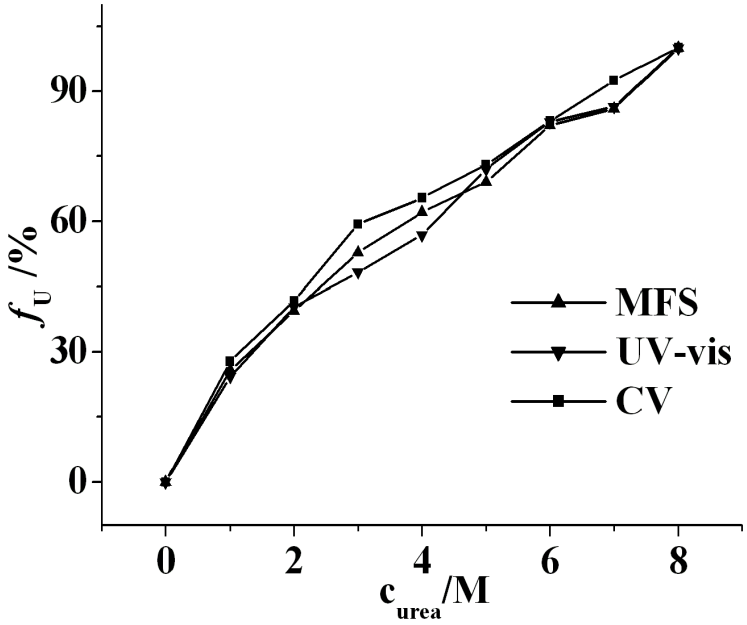

Fig. 5

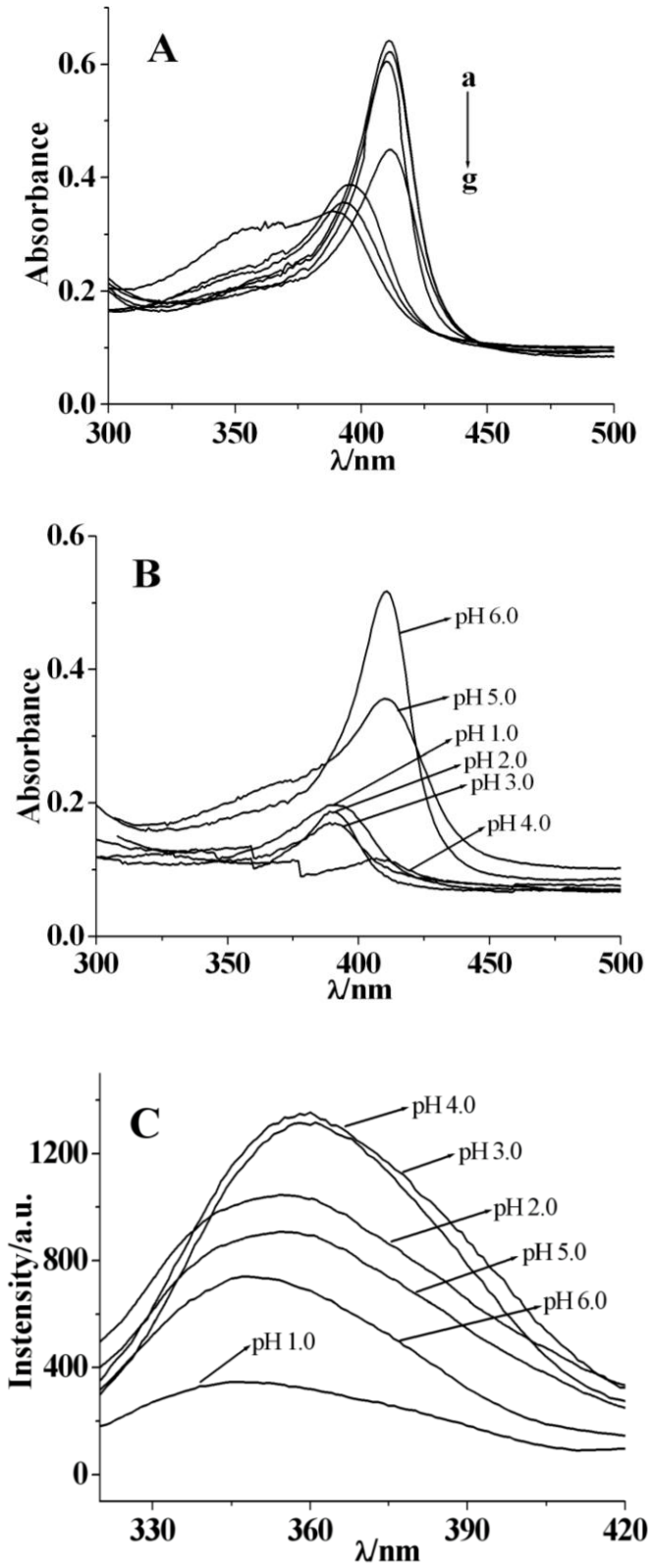

Fig. 6

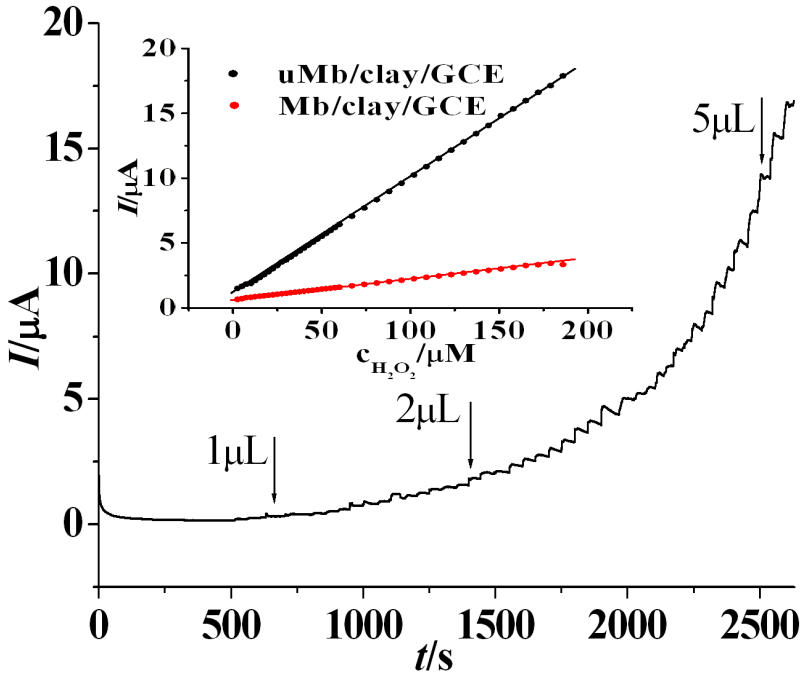

Fig. 7

Table 1

Characterization method	Electrochemistry	Trp fluorescence	UV-vis
m(kJ mol^{-2})	1.521	1.549	1.502
$\Delta G_{U,\ water}$(kJ mol^{-1})	12.78	13.05	13.21

Table 2

Sensors	Applied potential (V)	Linear range (mM)	Sensitivity μA mM^{-1} cm^{-2}	Detection limit (μM)	Literature
HRP/PTMSPA@GNR/ITO	–0.25	0.01 – 1	21	0.06	[51]
HRP-PANI-ClO_4^-/ITO	–	3 – 136	0.5638	–	[52]
Mb-ZnO/GCE	–0.339	0.0048 – 0.2	–	2	[53]
Hb-Fe_3O_4/GE/CCE	–0.3	0.0015 – 0.59	–	0.5	[54]
Nafion/Mb/Co/CILE	–0.473	0.01– 1.4	–	6	[55]
Chit-MWNTs/Mb/AgNPs/GCE	–0.3	0.025 – 0.2	–	1.02	[31]
SA/Hb/CILE	–0.25	1.0 – 100	–	1.0	[56]
Mb-[EMIM][BF4]-HA/GCE	–	2.0 – 270	–	0.6	[57]
SA/HRP/GCE	–	1.0 – 6.0	–	0.5	[58]
uMb/clay/GCE	–0.1	0.0008 –0.18	151.5	0.3	this work